



Article

Alkaloid Profiling, Anti-Enzymatic and Antiproliferative Activity of The Endemic Chilean Amaryllidaceae *Phycella cyrtanthoides*

Carlos Fernández-Galleguillos ^{1,*}, Javier Romero-Parra ², Adrián Puerta ³ , José M. Padrón ³ 
and Mario J. Simirgiotis ^{1,4,*} 

¹ Instituto de Farmacia, Facultad de Ciencias, Universidad Austral de Chile, Campus Isla Teja, Valdivia 5090000, Chile

² Departamento de Química Orgánica y Físicoquímica, Facultad de Ciencias Químicas y Farmacéuticas, Universidad de Chile, Olivos 1007, Casilla 233, Santiago 6640022, Chile; javier.romero@ciq.uchile.cl

³ BioLab, Instituto Universitario de Bio-Organica Antonio González (IUBO-AG), Universidad de La Laguna, 38206 La Laguna, Spain; apuerta@ull.es (A.P.); jmpadron@ull.es (J.M.P.)

⁴ Center for Interdisciplinary Studies on the Nervous System (CISNe), Universidad Austral de Chile, Valdivia 5090000, Chile

* Correspondence: carlos.fernandez@uach.cl (C.F.-G.); mario.simirgiotis@gmail.com or mario.simirgiotis@uach.cl (M.J.S.); Tel.: +56-57-2526910 (C.F.-G.); +56-63-63233257 (M.J.S.)

Abstract: This research aims to identify the alkaloid profile and to evaluate the enzyme inhibitory potential and antiproliferative effects of the Amaryllidaceae plant *Phycella cyrtanthoides*. The alkaloid extracts from bulbs and leaves were analyzed using ultrahigh performance liquid chromatography orbitrap mass spectrometry (UHPLC-Orbitrap-MS) analysis. A total of 70 alkaloids were detected in the *P. cyrtanthoides*' extracts. The enzyme inhibition potential against cholinesterases (AChE: acetylcholinesterase, and BChE butyrylcholinesterase) and tyrosinase were studied. Bulbs displayed the best IC₅₀ values against AChE (4.29 ± 0.03 µg/mL) and BChE (18.32 ± 0.03 µg/mL). These results were consistent with docking experiments with selected major compounds in the active sites of enzymes, while no activity was observed against tyrosinase enzyme. Antiproliferative effects were investigated against human cervical (HeLa), lung (A549, SW1573), colon (WiDr), and breast (HBL-100, T-47D) tumor cell lines. Bulbs and leaves were active in all cell lines (GI₅₀ < 2.5 µg/mL). These findings suggest that the endemic Chilean plant *P. cyrtanthoides* contains diverse types of bioactive alkaloids with antiproliferative activities and inhibitory effects with potential therapeutic applications for neurodegenerative diseases

Keywords: Amaryllidaceae alkaloids; *Phycella*; cholinesterase; tyrosinase; antiproliferative; UHPLC-MS



Citation: Fernández-Galleguillos, C.; Romero-Parra, J.; Puerta, A.; Padrón, J.M.; Simirgiotis, M.J. Alkaloid Profiling, Anti-Enzymatic and Antiproliferative Activity of The Endemic Chilean Amaryllidaceae *Phycella cyrtanthoides*. *Metabolites* **2022**, *12*, 188. <https://doi.org/10.3390/metabo12020188>

Academic Editor: Hirokazu Kawagishi

Received: 26 January 2022

Accepted: 14 February 2022

Published: 18 February 2022

Publisher's Note: MDPI stays neutral with regard to jurisdictional claims in published maps and institutional affiliations.



Copyright: © 2022 by the authors. Licensee MDPI, Basel, Switzerland. This article is an open access article distributed under the terms and conditions of the Creative Commons Attribution (CC BY) license (<https://creativecommons.org/licenses/by/4.0/>).

1. Introduction

Plants belonging to the Amaryllidaceae family are known for the biosynthesis of pharmacologically active alkaloids [1]. Traditionally, plants extracts of this family have been used as folk medicine for cancer in Ancient Greece, Asia, Africa, and Polynesia for a variety of ailments [2,3]. Galanthamine, an acetylcholinesterase (AChE) inhibitor, is well known for being the most important Amaryllidaceae alkaloid (AA) extracted and the first commercial natural product for the treatment of Alzheimer's disease (AD). The inhibition of AChE enzyme restored the levels of acetylcholine (ACh) in the postsynaptic neuronal membrane, improving the decline of cognitive function. Similarly, butyrylcholinesterase (BChE) enzyme also has an important function in cholinergic transmission and their levels are increased in AD [4]. Thus, several research groups have focused on finding new sources of bioactive alkaloids from Amaryllidaceae plants with cholinesterase inhibitory potential. On the other hand, these plants showed strong antiproliferative activity. Amaryllidaceae alkaloids, such as lycorine, haemantamine, pancratistatine, and montanine, have been

extensively screened for their antiproliferative effects [3,5–8]. Considering the structural variety and pharmacological properties of AAs, further studies aiming to identify and characterize active compounds would contribute to optimize their therapeutic applications. Different analytical methods have been used for the analysis of AAs, including thin layer chromatography (TLC) [9], capillary electrophoresis (CE) [10], and capillary-electrophoresis-MS (CE-MS) [11]. However, GC-MS and HPLC-MS have been widely and successfully employed in the analysis of AAs from plant sources [12–15]. Recently, ultra-high-performance liquid chromatography quadrupole time-of-flight mass spectrometry (UHPLC-QTOF-MS) has been used for the analysis of crude extracts in different *Lycoris* species [16].

The Amaryllidaceae family comprises 85 genera and approximately 1100 species, which are widely distributed in tropical, subtropical, and warm regions around the world [17]. In Chile, approximately 9 genera and 45 species have been described [18]. Additionally, some species belonging to the *Traubia*, *Placea* and *Phycella* genera have been cataloged as endemic [19,20].

Phycella genus is distributed in central Chile (from the Coquimbo to BíoBío region), where the following five species have been identified: *P. australis*, *P. scarlatina*, *P. herbetiana* (also present in Argentina), *P. brevituba*, and *P. cyrtanthoides* [21]. *P. cyrtanthoides* (local name: Añañuca de Fuego) is an endemic plant mainly found in the Metropolitana (Santiago) region and characterized by having a paraperigonium with fimbriae and six red flowers for umbel (Figure 1). To the best of our knowledge, no reports have been published that describe the chemistry and pharmacological properties of *P. cyrtanthoides* plants.



Figure 1. *Phycella cyrtanthoides* (Amaryllidaceae) plants.

In previous reports, the bulbs of *P. australis* were analyzed by GC-MS and showed a high content of haemantamine-type alkaloids. Pharmacological studies of the alkaloid fractions on human neuroblastoma cells suggested remarkable neuroprotective properties [22]. This study is one of the few regarding the chemical and pharmacological properties of the Chilean *Phycella*. The alkaloid profile and the AChE inhibitory potential from bulbs of the Argentinian *P. herbetiana* have also been investigated [23].

Considering the potential of AAs, we decided to explore the chemistry and pharmacological properties of *P. cyrtanthoides* for the first time using UHPLC-Orbitrap-MS. We screened the biological properties of the extracts based on enzymatic and cell models. The main objective of the present study is to investigate the alkaloid profile from the endemic *Phycella cyrtanthoides* (Amaryllidaceae) from bulbs and leaves organs. The alkaloid-rich

extracts were subjected to cholinesterase and tyrosinase inhibitory evaluation. Selected major compounds were studied by molecular docking to investigate intermolecular interactions with cholinesterase and tyrosinase enzymes. Antiproliferative activities were also evaluated using a panel of six solid tumor cells lines.

2. Materials and Methods

2.1. Chemicals

Ultra-pure water (<5 µg/L TOC) was obtained from a water system of purification (Milli-Q Merck Millipore, Chile). Methanol (HPLC grade) and formic acid (puriss. p.a. for mass spectrometry) from J. T. Baker (Phillipsburg, NJ, USA). Acetonitrile (HPLC grade) was from Merck (Santiago, Chile). 2,2-diphenyl-1-picrylhydrazyl (DPPH), gallic acid, DMSO, NaCl, MgCl₂, acetyl-thiocholine iodide (ATCI), butyryl-thiocholine chloride (BTCI), 5,5'-dithiobis (2-nitrobenzoic acid) (DTNB), sulforhodamine B (SRB), galanthamine, acetylcholinesterase (AChE), butyrylcholinesterase (BChE), and tyrosinase were purchased from Sigma-Aldrich Chem. Co. (St Louis, MO, USA). Lycorine hydrochloride was purchased from Sigma-Aldrich Chem. Co. (St Louis, MO, USA). Fetal calf serum (FCS) was purchased from Gibco (Grand Island, NY, USA). Trichloroacetic acid (TCA), glutamine, and gentamicin were purchased from Merck (Darmstadt, Germany).

2.2. Plant Material

Phycella cyrtanthoides was collected during the flowering state in the locality of Cachagua, Región de Valparaíso, Chile, in November of 2019 (22°34'26.7" S, 68°01'24.4" W). A voucher herbarium specimen (voucher number PC-52019) was deposited in the Laboratory of Natural Products of the Universidad Austral de Chile (Chile). The sample was authenticated by the botanist Jorge Macaya, University of Chile, Santiago, Chile. The entire plant was cleaned and separated into the different organs (Figure 2), dried, and stored without light, and then ground using an electric processor (Ursus Trotter, UT-PETRUS320) to prepare the extracts.



Figure 2. *Phycella cyrtanthoides*: entire plant (left), bulbs (middle), and leaves (right).

2.3. Extraction

Bulbs and leaves (100 g) were extracted three times with 100 mL MeOH using an ultrasonic water bath (UC-60A Biobase, Guanzhou, China) with a procedure similar to that usually reported to Amaryllidaceae alkaloids [24] with some modifications. Briefly, extracts were combined, filtered, and concentrated under reduced pressure. The raw extracts were acidified to pH 2 with H₂SO₄ (2% v/v) and extracted with Et₂O (3 × 30 mL). The aqueous solutions were basified with 25% NH₃·H₂O, up to pH 10. The alkaloids were extracted with EtOAc (3 × 50 mL). The organic layer was evaporated under reduced pressure to obtain the alkaloid extracts.

2.4. UHPLC–DAD–MS Instrument

The untargeted analysis of the alkaloid extracts was carried out using a UHPLC–high-resolution MS machine (Thermo Dionex Ultimate 3000 system with DAD detector controlled by Chromeleon 7.2 software hyphenated with a Thermo QExactive MS focus) operated in positive mode [25]. For the analysis, 5 mg of each partition extract were dissolved in 2 mL of methanol, filtered through a 200 µm polytetrafluoroethylene filter, and 10 µL were injected into the instrument. Data acquired were finally analyzed by Xcalibur 2.3 (Thermo Fisher).

2.5. LC Parameters and MS Parameters

Liquid chromatography was performed using a UHPLC C18 column (Acclaim, 150 × 4.6 mm ID, 2.5 µm; Thermo Fisher Scientific, Bremen, Germany) operated at 25 °C. The detection wavelengths were 280, 254, 330, and 354 nm, and photodiode array detector was set from 200 nm to 800 nm. A total of 1% formic acid aqueous solution was used as the mobile phase A, and the mobile phase B was acetonitrile. The gradient program was as follows: (0.00 min, 5% B); (5.00 min, 5% B); (10.00 min, 30% B); (15.00 min, 30% B); (20.00 min, 70% B); (25.00 min, 70% B); 35.00 min, 5% B) and 12 min for column prior to each injection equilibration before injections. The flow rate was 1.00 mL/min and the injection volume was 10 µL. Briefly, the parameters are as follows: sheath gas flow rate, 75 units; auxiliary gas unit flow rate, 20; capillary temperature, 400 °C; auxiliary gas heater temperature, 500 °C; spray voltage, 2500 V (for ESI); and S lens, RF level 30. Full scan data in positive mode were acquired at a resolving power of 70,000 FWHM at m/z 200. The mass scan range was between m/z 130–1000; automatic gain control (AGC) was set at 3×10^6 and the injection time of 200 ms. The chromatographic system was coupled to MS with a source II heated electro-nebulization ionization probe (HESI II). The nitrogen gas carrier (purity > 99.999%) was obtained from a Genius NM32LA (Peak Scientific, Billerica, MA, USA) generator and used as a collision and damping gas. Mass calibration for Orbitrap and HESI parameters were described previously [26].

2.6. Determination of Cholinesterase Inhibition

The inhibitory activity of *P. cyrtanthoides* extracts was evaluated by utilizing the Ellman's method as previously reported [27,28]. A sample solution (50 µL, 2 mg/mL) was mixed with 120 µL of 5,5-dithio-bis (2-nitrobenzoic) acid (DTNB) 0.3 mM, and AChE (0.26 U/mL, acetylcholinesterase from Electric eel), or BChE (0.26 U/mL, butyrylcholinesterase from horse serum) solution (25 µL) in Tris-HCl buffer 50 mM (pH = 8.0) in a 96-well microplate and incubated for 20 min at 37 °C. The reaction was initiated by the addition of 25 µL of acetylthiocholine iodide (ATCI) 1.5 mM or butyrylthiocholine chloride (BTCl) 1.5 mM. A blank was prepared to all reaction reagents without enzymes solution. The absorbances were recorded at three times at 405 nm during 30 min at 37 °C using microplate reader (Synergy HTX Multi-Mode). Galanthamine hydrobromide was used as a positive control. The cholinesterase inhibitory activity was expressed as IC₅₀ (µg/mL, concentration range 0.5 to 50 µg/mL). All data were recorded in triplicate.

2.7. Determination of Tyrosinase Inhibition

Tyrosinase inhibitory activity was evaluated by utilizing the dopachrome method as previously reported [26]. *P. cyrtanthoides* extract solution (20 µL, 2 mg/mL) was mixed with Mushroom tyrosinase solution (100 unit/mL, 40 µL) and phosphate buffer 0.067 M (30 µL, pH = 6.8) in a 96-well microplate and incubated for 15 min at 30 °C. The reaction was initiated with the addition of 40 µL L-DOPA 2.5 mM and the mixture was incubated for 15 min at 25 °C. A blank was prepared to all reaction reagents without enzyme. The sample and blank absorbances were recorded at 492 nm using a microplate reader (Synergy TM HT Multi-Mode). Kojic acid was used as a positive control. The tyrosinase inhibitory activity was expressed as IC₅₀ (µg/mL, concentration range 31.25 to 250 µg/mL). All data were recorded in triplicate.

2.8. Docking Assays

Docking simulations were carried out for selected major alkaloids, shown in Figure S1 (Supplementary Material), obtained from *Phycella cyrtanthoides* leaves or bulbs extracts. The geometries and partial charges of each alkaloid were fully optimized using the DFT/B3LYP method with standard basis set 6-311G/+dp [29,30] in Gaussian 09W software. Crystallographic enzyme structures of *Torpedo Californica* acetylcholinesterase (TcAChE; PDBID: 1DX6 code) [31], and human butyrylcholinesterase (hBuChE; PDBID: 4BDS code) [32] were downloaded from the Protein Data Bank RCSB PDB [33] (for full description, see Supplementary Material).

2.9. Antiproliferative Activity

Antiproliferative activity was evaluated using human solid tumor cell lines. Cells were inoculated onto 96-well plates using 100 μ L per well at densities of 2500 (A549, HBL-100, and HeLa) and 5000 (SW1573, T-47D, and WiDr) cells per well. Extract solutions dispersed in water were dissolved in DMSO at 400 times the final maximum test concentration (250 μ g/mL). Control cells were exposed to an equivalent concentration of DMSO (0.25% *v/v*, negative control). The extracts were tested in triplicate at concentrations ranging from 250 to 2.5 μ g/mL. Treatment with compounds started on day 1 after plating. Incubation time with compounds was 48 h, after which cells were precipitated with ice-cold trichloroacetic acid (TCA) (50% *w/v*, 25 μ L) during 60 min at 4 °C. Then, the sulforhodamine B (SRB) assay was performed. The optical density (OD) was measured at 530 nm using BioTek PowerWave XS microplate reader. The results were expressed as GI₅₀ values (μ g /mL, calculated according to NCI formulas).

2.10. Statistical Analysis

The results obtained from these experiments were repeated five times and expressed as mean \pm standard error of mean. Statistical analysis of the data was performed using analysis of variance (two-way ANOVA) where applicable followed by post hoc Bonferroni test. In addition, the determination of the sensitivity (EC₅₀ or IC₅₀) was performed using nonlinear regression (sigmoidal) via origin Pro 9.0 software package (Origin lab Corporation, Northampton, MA, USA). Statistical significance was set at $p < 0.05$.

3. Results and Discussion

3.1. Alkaloid Profiling of *Phycella Cyrtanthoides* Extracts

In the present work, the alkaloid profiling of bulbs and leaves from the methanolic extracts of *Phycella cyrtanthoides* was investigated. This is the first report concerning the alkaloid profiling of *P. cyrtanthoides*. In total, 70 alkaloids were detected by UHPLC-PDA-Orbitrap-Mass Spectrometry, among them 47 were tentatively identified and 23 could not be identified using the techniques described herein (see Table 1, and Figure 3). One alkaloid was identified by spiking experiments with available standards (lycorine hydrochloride) using positive mode of detection. The generation of molecular formulas was performed using high resolution accurate mass analysis (HRAM) and matching with the isotopic pattern. Finally, analyses were confirmed using MS/MS data, fragmentation pattern, database of MassBank of North America (MoNA), and the published literature.

Lycorin and homolycorine-type alkaloids were the most common alkaloids identified on the extracts. In addition, crinine, haemanthamine, tazettine and belladine-type alkaloids were also detected. The distribution of the alkaloids in *P. cyrtanthoides* varied according to the organs. However, a total of nine alkaloids (lycorine, pseudolycorine, hippeastrine, candimine, haemanthamine, vittatine, 7-methoxy-*O*-methyllycorine, 5-methyl-2-epihippamine and 1-*O*-acetylbuphanamine) were found both in bulbs and leaves (Figure 4). The representative interpretations among the identified alkaloids are discussed below.

Table 1. Ultrahigh performance liquid chromatography orbitrap mass spectrometry (UHPLC-Orbitrap-MS) identification of *Phycella cyrtanthoides*.

Peak	UV Max	Tentative Identification Name (AA-Type)	Elemental Composition [M+H] ⁺	Rt	Theoretical Mass (m/z)	Measured Mass (m/z)	Accuracy (ppm)	MSn Ions (ppm)	Organs
1	236–281	2-Hydroxyalbomaculine (homolycorine-type)	C ₁₉ H ₂₄ O ₆ N ⁺	0.86	362.15981	362.13348	−72.719	274.14774, 251.09735, 214.06267, 199.07582, 165.07063, 121.06544, 107.04959	L
2	231–248-271–307	Tazettine isomer (tazettine-type)	C ₁₈ H ₂₂ O ₅ N ⁺	1.37	332.14925	332.15756	25.020	316.12589, 274.14835, 247.12236, 228.14095, 181.06543, 152.06271, 115.05478, 107.04965	L
3	233–247-306	Powelline (crinine-type)	C ₁₇ H ₂₀ O ₄ N ⁺	2.06	302.13868	302.14523	21.663	284.13364, 274.14798, 251.09767, 228.06763, 181.06557, 165.07068, 127.05473, 115.05476,	L
4	236–286	Lycorine * (lycorine-type)	C ₁₆ H ₁₈ O ₄ N ⁺	3.07	288.12303	288.12869	19.628	286.11295, 239.05540, 194.11844, 166.12335, 147.04440, 119.04981, 103.05488	B; L
5	235–283	Pseudolycorine (lycorine-type)	C ₁₆ H ₂₀ O ₄ N ⁺	3.11	290.13923	290.14432	19.423	244.09990, 214.08778, 177.26830, 153.07031, 152.06248, 147.04427, 119.04977, 112.91312	B; L
6	233–278	Hippeastrine isomers (homolycorine-type)	C ₁₇ H ₁₈ O ₅ N ⁺	3.25	316.11850	316.12579	25.689	298.11389, 290.14404, 280.10153, 274.14795, 191.03445, 166.12321, 121.06518	B; L
7	231–276	Hippeastrine isomers (homolycorine-type)	C ₁₇ H ₁₈ O ₅ N ⁺	4.54	316.11850	316.12579	24.803	290.14407, 274.14798, 191.03456, 166.12329, 121.06531	L
8	232–278	Hippeastrine isomers (homolycorine-type)	C ₁₇ H ₁₈ O ₅ N ⁺	4.59	316.11850	316.12616	25.973	291.14764, 274.14828, 191.03468, 247.12253, 166.12341, 121.06541	B
9	233–289	Pluviine (lycorine-type)	C ₁₇ H ₂₂ O ₃ N ⁺	5.35	288.15942	288.12869	19.628	275.25861, 270.11700, 240.06802, 194.09659, 165.07004, 147.04448, 119.04977	B
10	232–289	Dihydrolycorine (lycorine-type)	C ₁₆ H ₂₀ O ₄ N ⁺	6.59	290.13923	290.14432	19.423	272.13245, 257.15308, 220.12132, 167.11861, 152.06258, 149.06068	B
11	233–290	3-O-methyl-epimacowine (crinine-type)	C ₁₆ H ₁₈ O ₄ N ⁺	6.73	288.12358	288.12872	19.732	193.65796, 179.76768, 153.07051, 128.55969, 115.05492, 109.22836	B
12	231–277-310	11-O-methylcrinamine (crinine-type)	C ₁₈ H ₂₂ O ₄ N ⁺	6.84	316.15433	316.12589	−89.979	631.24774 (2M ⁺), 274.14807, 228.14088, 182.11839, 121.06535	L
13	231–277	3-Hydroxydihydrocaranine (lycorine-type)	C ₁₆ H ₂₀ O ₄ N ⁺	7.74	290.13868	290.14420	19.940	268.67581, 239.88618, 167.34416, 137.10796, 111.88570, 107.48717	B

Table 1. Cont.

Peak	UV Max	Tentative Identification Name (AA-Type)	Elemental Composition [M+H] ⁺	Rt	Theoretical Mass (m/z)	Measured Mass (m/z)	Accuracy (ppm)	MSn Ions (ppm)	Organs
14	232–278	<i>epi</i> -Zephyranthine isomers (lycorine- type)	C ₁₆ H ₂₀ O ₄ N ⁺	8.34	290.13868	290.14413	18.768	272.13232, 262.11163, 244.09996, 214.08743, 181.06534, 169.06546, 147.04451, 120.08131, 118.06568	L
15	232–278	<i>epi</i> -Zephyranthine isomers (lycorine- type)	C ₁₆ H ₂₀ O ₄ N ⁺	8.81	290.13868	290.14435	19.526	272.13245, 268.74606, 181.17052, 170.64424, 148.16725, 129.39676, 118.06547	B
16	232–275	Hippeastrine isomers (homolycorine-type)	C ₁₇ H ₁₈ O ₅ N ⁺	9.67	316.11850	316.12579	24.80	298.11267, 290.14447, 274.14795, 191.03447, 166.12320, 121.06516	L
17	232–275	Hippeastrine isomers (homolycorine-type)	C ₁₇ H ₁₈ O ₅ N ⁺	10.09	316.11850	316.12610	−22.476	288.12851, 274.14813, 191.03467, 166.12337, 137.10789, 124.07613	B
18	235–282-314	Candimine (homolycorine-type)	C ₁₈ H ₂₀ O ₆ N ⁺	10.75	346.12906	346.13831	28.301	316.12576, 288.12836, 274.14810, 228.14084, 155.15477, 138.05533, 121.06532	B; L
19	234–385	8- <i>O</i> -demethylmaritidine (haemanthamine-type)	C ₁₆ H ₂₀ O ₃ N ⁺	11.39	274.14377	274.14804	15.576	267.06967, 223.07715, 191.03459, 177.01894, 149.02383, 121.06531, 107.04959	L
20	232–273	Haemanthamine (haemanthamine-type)	C ₁₇ H ₂₀ O ₄ N ⁺	11.78	302.13923	302.14548	22.490	289.13168, 272.13251, 228.14088, 183.57773, 180.10258, 167.11855, 161.10791, 144.08138	B; L
21	235–282	5-Methyl-epimethylpseudolycorine (lycorine-type)	C ₁₈ H ₂₄ O ₄ N ⁺	11.89	318.17053	318.17819	25.788	287.12823, 162.06857, 147.04459, 125.98681, 115.05488, 103.05471	B
22	241–325	2α-Methoxy-6- <i>O</i> -ethyloduline (homolycorine-type)	C ₂₀ H ₂₆ O ₅ N ⁺	12.16	360.18110	360.19092	28.792	330.14169, 274.14807, 270.11676, 228.14082, 153.10274, 151.07596, 121.06521	L
23	240–291	Vittatine (haemanthamine- type)	C ₁₆ H ₁₈ O ₃ N ⁺	12.43	272.12867	272.13257	16.242	268.10175, 247.12251, 199.21875, 180.10249, 167.99812, 153.13918, 121.06526, 115.05503	B; L
24	233–288	10-Norpluviine (lycorine-type)	C ₁₆ H ₂₀ O ₃ N ⁺	12.63	274.14432	274.14813	15.904	274.14813, 256.13666, 228.14076, 175.03946, 147.04443, 121.06533, 118.06563, 102.03407	L

Table 1. Cont.

Peak	UV Max	Tentative Identification Name (AA-Type)	Elemental Composition [M+H] ⁺	Rt	Theoretical Mass (m/z)	Measured Mass (m/z)	Accuracy (ppm)	MSn Ions (ppm)	Organs
25	236–287	Kirkine (lycorine-type)	C ₁₆ H ₂₀ O ₃ N ⁺	12.73	274.14432	274.14822	16.232	270.11679, 256.13672, 231.15173, 228.07106, 197.16562, 175.03972, 120.08125, 118.06559	B
26	232–272	Albomaculine (homolycorine-type)	C ₁₉ H ₂₄ O ₅ N ⁺	12.87	346.16490	346.17456	27.994	320.15652, 304.16083, 274.14795, 193.05043, 180.10242, 178.06317, 152.06268, 103.05467	L
27	232–256-309	3-Epimacronine (tazettine-type)	C ₁₈ H ₂₀ O ₅ N ⁺	13.05	330.13415	330.14191	25.173	326.09451, 316.12592, 247.12227, 231.15181, 202.13469, 167.15497, 144.08133, 111.09221	B
28	234–252	10-O-methylpseudolycorine (lycorine-type)	C ₁₇ H ₂₂ O ₄ N ⁺	13.12	304.15488	304.16098	21.848	304.16074, 276.12741, 258.11655, 193.05020, 178.06328, 165.07066, 147.04482, 125.08409, 118.06564	L
29	232–271	Aknadicine	C ₁₉ H ₂₄ O ₅ N ⁺	13.29	346.16545	346.17526	29.929	316.12640, 304.16125, 193.05049, 178.06313, 125.08411, 121.06541, 110.06061	L
30	248–271	3-O-Acetylnarcissidine (lycorine-type)	C ₂₀ H ₂₆ O ₆ N ⁺	13.43	376.17601	376.18796	33.217	316.12589, 304.16135, 258.11682, 193.05042, 165.07048, 153.07048, 147.04456, 125.08416, 118.06568	L
31	238–284	10-O-Dimethylgalanthine (lycorine-type)	C ₁₇ H ₂₂ O ₄ N ⁺	13.48	304.15488	304.16119	22.539	274.14847, 266.08557, 258.11697, 191.15506, 167.15486, 125.98666, 118.06574	B
32	248–271	7-Methoxy-O-methyllycorenine (homolycorine-type)	C ₂₀ H ₂₈ O ₅ N ⁺	13.75	362.19675	362.20648	29.405	346.13885, 330.14188, 247.12267, 221.16689, 191.15508, 167.01363	B; L
33	238–271	Unknown alkaloid	C ₂₄ H ₂₆ O ₄ N ⁺	13.97	392.18618	392.18298	−6.769	376.18741, 344.15909, 304.16098, 252.10530, 212.14474, 180.10254	L
34	249–278	Unknown alkaloid	C ₂₀ H ₂₄ O ₄ N ⁺	14.05	342.17053	342.17990	28.977	337.19955, 316.12595, 259.18481, 247.12242, 194.11845, 144.08136	B
35	241–287	Unknown alkaloid	C ₁₉ H ₂₂ O ₅ N ⁺	14.24	344.16183	344.15912	28.681	337.19943, 316.16238, 282.11783, 227.08345, 191.14377, 110.02042	L

Table 1. Cont.

Peak	UV Max	Tentative Identification Name (AA-Type)	Elemental Composition [M+H] ⁺	Rt	Theoretical Mass (m/z)	Measured Mass (m/z)	Accuracy (ppm)	MSn Ions (ppm)	Organs
36	248–284	Homolycorine (homolycorine-type)	C ₁₈ H ₂₂ O ₄ N ⁺	14.29	316.15488	316.16257	−22.206	312.16776, 284.18124, 272.13272, 251.15782, 201.13953, 181.17062, 125.98682, 110.02058	B
37	249–284	Unknown alkaloid	C ₁₄ H ₃₀ O ₉ N ⁺	14.42	356.19151	356.19595	12.471	226.28473, 201.05020, 143.05002, 115.05481, 108.08139	B; L
38	249–282	Unknown alkaloid	C ₁₈ H ₃₄ O ₇ N ⁺	14.60	376.23298	376.22391	−24.105	356.19583, 322.15192, 240.15221, 181.17058, 167.01340, 125.98679	B
39	242	Unknown alkaloid	C ₁₈ H ₃₄ O ₈ N ⁺	14.68	392.22789	392.21906	−22.522	374.17166, 346.17444, 290.15924, 197.11798, 150.09190, 121.06519	B; L
40	243	Unknown alkaloid	C ₂₄ H ₂₄ O ₅ N ⁺	14.85	406.16490	406.16412	−7.395	392.21921, 346.10187, 290.15942, 274.14810, 211.17101, 197.11813, 179.10728	L
41	253–282	5-methyl-2-epihippamine isomers (lycorine-type)	C ₁₈ H ₂₂ O ₄ N ⁺	14.99	316.15433	316.12613	25.878	284.18137, 272.13257, 254.16881, 247.12253, 197.08179, 144.08141, 125.98682, 111.09224	B; L
42	252–276	Unknown alkaloid	C ₁₉ H ₃₀ O ₆ N ⁺	15.37	368.20676	368.19748	32.171	316.12601, 249.14214, 228.14104, 209.20259, 167.01352, 110.02060	B
43	252–278	Unknown alkaloid	C ₂₈ H ₃₃ O ₅ N ⁺	15.53	463.23532	463.24121	12.705	449.26157, 431.21402, 346.13846, 249.14217, 225.12744, 163.07600	B
44	251–301	3-O-methylnarcissidine (lycorine-type)	C ₁₉ H ₂₆ O ₅ N ⁺	15.85	348.18055	348.19052	28.636	346.17471, 274.14804, 197.11795, 171.14987, 138.09195, 121.06521	L
45	250–280	Unknown alkaloid	C ₂₆ H ₃₂ O ₃ N ⁺	15.96	406.23767	406.23715	−1.281	346.13843, 316.12604, 247.12244, 203.11884, 144.08141,	B
46	252–297	2-O-acetyl-4-O-methyllicorine (lycorine-type)	C ₁₉ H ₂₂ O ₆ N ⁺	16.33	360.14471	360.15427	28.061	314.14539, 267.12448, 247.12241, 211.07701, 171.14987, 121.06534, 103.05473	L
47	253–283	Jonquailine (tazettine-type)	C ₁₉ H ₂₄ O ₅ N ⁺	16.45	346.16490	346.13846	−76.384	321.20441, 314.14566, 288.05582, 247.12248, 171.14989, 102.03439	B
48	261–305	Unknown alkaloid	C ₁₉ H ₂₂ O ₆ N ⁺	16.63	360.14416	360.15417	27.783	344.12250, 326.14676, 316.12579, 304.16077, 247.12231, 180.10242, 164.10765	L
49	252–282	Unknown alkaloid	C ₂₇ H ₃₃ O ₃ N ⁺	16.76	419.24550	419.24805	6.093	398.21057, 346.13849, 316.12604, 268.13763, 210.12157, 121.06532	B

Table 1. Cont.

Peak	UV Max	Tentative Identification Name (AA-Type)	Elemental Composition [M+H] ⁺	Rt	Theoretical Mass (m/z)	Measured Mass (m/z)	Accuracy (ppm)	MSn Ions (ppm)	Organs
50	250–275	Bulbocapnine (isoquinoline alkaloid)	C ₁₉ H ₂₀ O ₄ N ⁺	16.85	326.13923	326.14673	24.668	282.08136, 274.14810, 240.13322, 225.15038, 207.13930, 138.09189, 121.06530	L
51	253–278	Unknown alkaloid	C ₂₁ H ₃₂ O ₄ N ⁺	17.18	362.23258	362.22394	−23.866	360.21735, 316.12598, 247.12244, 167.01346, 102.03439	B
52	254–297	Unknown alkaloid	C ₁₈ H ₂₆ O ₇ N ⁺	17.39	368.17038	368.17639	16.328	346.17471, 316.12595, 304.16098, 274.14807, 164.10770, 102.03436	L
53	253–302	Nerinine (homolycorine-type)	C ₁₉ H ₂₅ O ₅ N ⁺	18.34	347.17272	347.17801	59.168	346.17453, 316.12576, 247.14180, 197.11798, 152.10750, 102.03431	L
54	242–277	Unknown alkaloid	C ₂₄ H ₁₆ O ₃ N ⁺	18.82	366.11247	366.10648	28.525	344.12265, 316.12579, 274.14801, 256.06381, 167.01337, 110.02050, 102.03431	L
55	285–310	1-O-acetylcaranine (lycorine-type)	C ₁₈ H ₂₀ O ₄ N ⁺	19.24	314.13868	314.10910	−94.186	304.16092, 278.08636, 270.15344, 252.10562, 247.12234, 226.18208, 191.03456, 102.03433	L
56	266–309-356	Unknown alkaloid	C ₂₃ H ₂₀ O ₃ N ⁺	19.41	358.14377	358.13867	−14.240	336.09265, 314.10925, 278.08649, 191.03464, 102.03435	L
57	251–282	Unknown alkaloid	C ₁₄ H ₂₁ O ₃ N ⁺	20.32	251.15159	251.15793	25.223	250.14595, 228.14110, 186.09221, 167.01358, 102.03442	B
58	253–327	Carltonine A (belladine-type)	C ₂₇ H ₃₃ O ₃ N ₂ ⁺	20.44	433.24857	433.26575	39.654	399.18460, 388.15140, 376.18735, 316.12582, 247.12230, 167.01335, 122.54755	L
59	251–278	Unknown alkaloid	C ₂₇ H ₃₈ O ₆ N ⁺	20.79	472.26936	472.28061	23.811	449.26141, 429.29208, 346.13840, 247.12242, 144.08139	B; L
60	245–284	Unknown alkaloid	C ₂₄ H ₂₂ O ₄ N ⁺	21.06	388.15433	388.15140	−7.561	330.10541, 316.12585, 274.14807, 225.55421, 187.12723, 167.01343	B; L
61	251–285	Unknown alkaloid	C ₁₅ H ₂₇ O ₃ N ⁺	21.27	269.19909	269.20554	25.983	267.19000, 247.12218, 235.17180, 184.10028, 150.09189, 121.06524	B; L
62	252–281	Unknown alkaloid	C ₂₀ H ₃₃ O ₆ N ⁺	21.38	383.23024	383.23532	13.258	352.34933, 316.12595, 269.20566, 228.14091, 221.15578, 144.08133	B
63	252–297	11-Oxo-haemanthamine (haemanthamine-type)	C ₁₇ H ₁₈ O ₄ N ⁺	21.46	300.12303	300.12955	21.709	277.19623, 269.20547, 240.25401, 239.25075, 211.08781, 180.10248, 102.03432	L

Table 1. Cont.

Peak	UV Max	Tentative Identification Name (AA-Type)	Elemental Composition [M+H] ⁺	Rt	Theoretical Mass (m/z)	Measured Mass (m/z)	Accuracy (ppm)	MSn Ions (ppm)	Organs
64	253–282	Unknown alkaloid	C ₁₄ H ₂₁ O ₃ N ⁺	21.89	251.15159	251.15799	25.462	247.12265, 212.14493, 186.12865, 167.01361, 144.08147, 102.03445	B
65	255–302	1-O-acetylbuphanamine (crinine-type)	C ₁₉ H ₂₂ O ₅ N ⁺	22.23	344.14925	344.15903	−14.851	294.11795, 274.14795, 197.11797, 181.12305, 174.12837, 138.09187	B; L
66	257	11-Acetylbambinine (crinine-type)	C ₂₀ H ₂₄ O ₆ N ⁺	22.33	374.16036	374.17181	32.060	358.13858, 324.13116, 304.16089, 197.11806, 174.12848, 151.11229, 121.06525	B; L
67	255–306	Maritidine (haemanthamine type)	C ₁₇ H ₂₂ O ₃ N ⁺	22.78	288.15942	288.12863	27.502	244.13684, 216.14043, 191.03470, 167.01357, 122.54771, 102.03446	B; L
68	257–296	9-Norpluviine (lycorine-type)	C ₁₆ H ₂₀ O ₃ N ⁺	23.05	274.14432	274.14798	15.357	274.14798, 256.26694, 230.25032, 228.27116, 191.03436, 174.12823, 147.18108, 121.06519, 102.03426	L
69	258	5-Methylpseudolycorine (lycorine-type)	C ₁₇ H ₂₂ O ₄ N ⁺	24.22	304.15433	304.16098	21.848	258.28345, 242.28685, 228.27103, 174.12837, 151.11229, 102.03432	L
70	257–292	Unknown alkaloid	C ₂₄ H ₂₆ O ₃ N ⁺	24.37	376.19072	376.18744	−8.720	352.34924, 274.14795, 258.28336, 174.12845, 166.11258, 146.09694, 132.08127	L

Abbreviations: L = leaves; B = bulbs; RT = retention time; * = identified using authentic compounds.

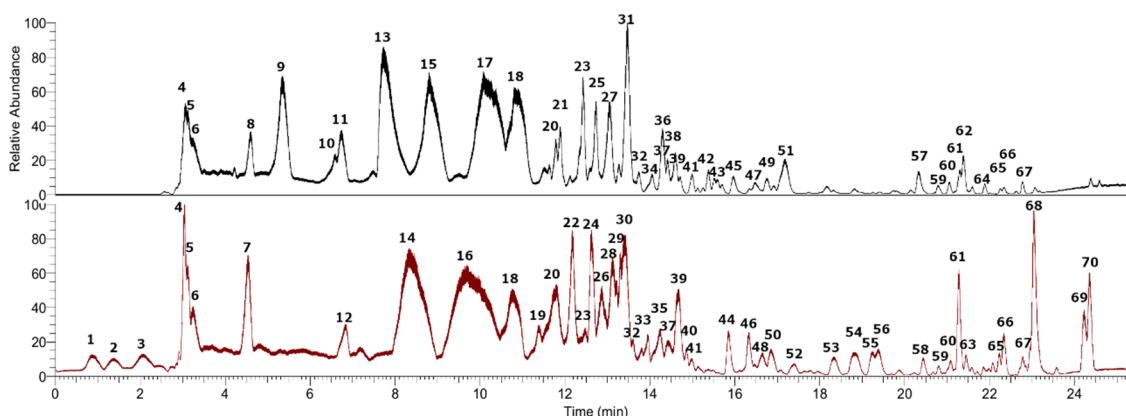


Figure 3. UHPLC chromatogram of *Phycella cyrthanthoides* bulbs (black) and leaves (red) in positive mode.

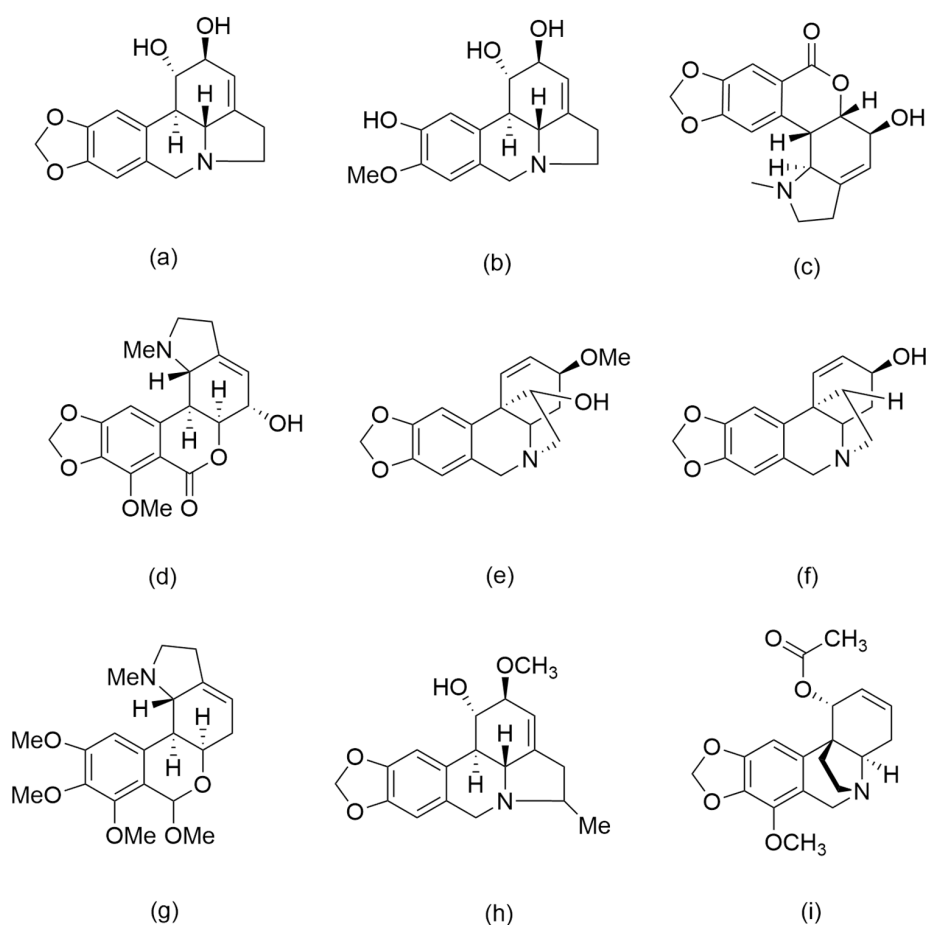


Figure 4. Lycorine (a), pseudolycorine (b), hippastrine (c), candimine (d), haemanthamine (e), vittatine (f), 7-methoxy-*O*-methyllycorenine (g), 5-methyl-2-epihippamine (h) and 1-*O*-acetylbuphanamine (i).

Peak 1 with a $[M+H]^+$ ion at $m/z = 362.13348$ was identified as 2-hydroxyalbomaculine, previously isolated from the aerial parts of *Zephyranthes candida* [34]. Peak 2 was identified as tazettine ($C_{18}H_{22}O_5N^+$, 332.15756), which was reported previously from bulbs of Chilean *Phycella australis* [22] and the Argentinian *Phycella herbetiana* [23]. Peak 3 was identified as powelline ($C_{17}H_{20}O_4N^+$, 302.14523) based on the formation of $[M+H-H_2O]^+$ ion at $m/z = 284.13364$, suggesting the presence of hydroxyl group at C-3 [35]. Peak 4 with a $[M+H]^+$ ion at $m/z = 288.12869$ and diagnostic fragments formed after the retro Diels–Alder rearrangements (RDAr) at $m/z = 239.05540$, $m/z = 147.04440$, and $m/z = 119.04981$ was

identified as lycorine ($C_{16}H_{18}O_4N^+$) [23]; peak 5 with a $m/z = 290.14432$ was identified as pseudolycorine ($C_{16}H_{20}O_4N^+$) according to the fragmentation data [36] and previously reported from *P. australis* [22] and *P. herbetiana* [23].

Peak 6 with a $[M+H]^+$ ion at $m/z = 316.12579$ showed diagnostic fragments detected at $m/z = 298.11389$ (loss of H_2O), $m/z = 280.10153$ (loss of $2H_2O$) and $m/z = 191.03445$ (formed by RDAr) in agreements with hippeastrine ($C_{17}H_{18}O_5N^+$). Peak 7 and peak 8 produced the same fragmentation ions and were identified as hippeastrine isomers [37]. Peak 9 was identified as pluviine ($C_{17}H_{22}O_3N^+$, 288.12869), peak 10 as dihydrolycorine ($C_{16}H_{20}O_4N^+$, 290.14432) and also detected on *Phycella australis* [22], and peak 11 as 3-O-methyl-epimacowine ($C_{16}H_{18}O_4N^+$, 288.12872), previously identified from the bulbs of the Brazilian *Hippeastrum calyptatum* [38]. Peak 12 with a $[M+H]^+$ ion at $m/z = 316.12589$ was identified as 11-O-methylcrinamine [39], peak 13 as 3-hydroxydihydrocaranine ($C_{16}H_{20}O_4N^+$, 290.14420), and peaks 14 and 15 were proposed as epi-zephyranthine isomers ($C_{16}H_{20}O_4N^+$, 290.14420). Peak 16 and peak 17 were identified as hippeastrine isomers, while peak 18 with a $[M+H]^+$ ion at $m/z = 346.13831$ was identified as candimine, previously reported from *Hippeastrum morelianum* bulbs [40]. Peak 19 with a $[M+H]^+$ ion at $m/z = 274.14804$ was identified as 8-O-demethylmaritidine [41] and peak 20 with fragments at $m/z = 272.13251$, $m/z = 180.10258$ and $m/z = 167.11855$ was identified as haemanthamine ($C_{17}H_{20}O_4N^+$, 302.14548). Haemanthamine was also identified on *Phycella australis* [22].

Peak 21 was identified as 5-methyl-epimethylpseudolycorine [16], peak 22 as 2 α -methoxy-6-O-ethyloduline previously isolated from *Lycoris radiata* [42], peak 23 with diagnostic fragments at $m/z = 180.10249$ and $m/z = 167.01340$ was proposed as vittatine ($C_{16}H_{18}O_3N^+$, 272.13257) previously detected from *P. australis* [22] and *P. herbetiana* [23], peak 24 as 10-norpluviine ($C_{16}H_{20}O_3N^+$, 274.14432) [16], peak 25 as kirkinine ($C_{16}H_{20}O_3N^+$, 274.14822) [16], and peak 26 as albomaculine ($C_{19}H_{24}O_5N^+$, 346.17456) [43].

Peak 27 with a $[M+H]^+$ ion at $m/z = 330.14191$ was identified as 3-epimacronine also found on *P. australis* [22], peak 28 as 10-O-methylpseudolycorine, peak 29 as the isoquinoline alkaloids aknadine detected on bulbs of *Narcissus tazetta* [44] and peak 30 as 3-O-acetylnarcissidine [45]. Peak 31 was identified as 10-O-dimethylgalanthine [16], peak 32 as 7-methoxy-O-methyllycorenine previously isolated from Brazilian *Hippeastrum aulicum* [38], peak 36 was identified as homolycorine [46], and peak 41 was identified as 5-methyl-2-epihippamine, peak 44 as 3-O-methylnarcissidine [47], peak 46 as 2-O-acetyl-4-O-methyllycorine [16], peak 47 as jonquiline [48], and peak 50 as the classical isoquinoline bulbocapnine. These alkaloids have been isolated previously from *Galanthus nivalis* [49] and detected recently from bulbs of *Narcissus tazetta* [44]. Peak 53 was identified as nerinine detected in some Chilean *Rhodophiala* species [12], peak 55 was identified as 1-O-acetylcaranine [50], and peak 58 was identified as the belladine-type alkaloid carltonine A isolated from the bulbs of *Narcissus pseudonarcissus* cv. Carlton [51]. Peak 63 with a $[M+H]^+$ ion at $m/z = 300.12955$ was identified as 11-oxo-haemanthamine [38], peak 65 as 1-O-acetylbuphanamine isolated from the bulbs of *Boophone disticha* [52], and peak 66 as 11-acetyllambelline [53]. Peak 67 with a $[M+H]^+$ ion at $m/z = 288.12863$ was identified as maritidine, and was detected previously from *P. australis* bulbs [22], peaks 68 and 69 were proposed as 9-norpluviine [16], and 5-methylpseudolycorine [16].

3.2. Enzyme Inhibition Studies

Phycella cyrtanthoides bulbs and leaves alkaloid extracts were evaluated *in vitro* for acetylcholinesterase, butyrylcholinesterase and tyrosinase inhibitory effects (Table 2, expressed as IC_{50} values). Bulbs and leaves were active against AChE and BChE. Bulbs showed the highest inhibitory effects compared to leaves with IC_{50} values for AChE of 4.29 ± 0.04 and for BChE of 18.32 ± 0.03 $\mu\text{g/mL}$. *P. cyrtanthoides* bulbs were more active than Chilean *P. australis* bulbs ($IC_{50} = 80.12 \pm 1.03$ $\mu\text{g/mL}$) [22], while the Argentinian *P. herbetiana* bulbs showed strong inhibitory activity against AChE ($IC_{50} = 1.2 \pm 0.12$ $\mu\text{g/mL}$) [23]. No results regarding BChE inhibitory activity have been reported for other *Phycella* species. Conversely, no activity was detected against tyrosinase enzyme on the bulbs and leaves

of the alkaloid extract of *P. cyrtanthoides*. These results are in agreement with previous studies using isolated and alkaloid fractions [54], since the presence of phenolic groups has positive effects on the inhibitory activity due to the chelating properties of metals such as copper [26].

Table 2. Enzymatic inhibitory activity of *Phycella cyrtanthoides* alkaloid extracts.

Assay	AChE Inhibition IC ₅₀ (µg/mL)	BChE Inhibition IC ₅₀ (µg/mL)	Tyrosinase Inhibition IC ₅₀ (µg/mL)
<i>P. cyrtanthoides</i> bulbs	4.29 ± 0.04	18.32 ± 0.03	ND
<i>P. cyrtanthoides</i> leaves	8.66 ± 0.03	37.70 ± 0.02	ND
Galanthamine	0.55 ± 0.03	3.82 ± 0.02	-
Kojic acid	-	-	0.76 ± 0.05

All values are expressed as means ± SD (n = 3). Abbreviations: AChE, acetylcholinesterase; BChE, butyrylcholinesterase; ND, not detected (>250 µg/mL).

3.3. Docking Studies

All compounds subjected to docking assays in the *Torpedo californica* acetylcholinesterase (*TcAChE*) catalytic site and human butyrylcholinesterase (*hBChE*) catalytic site turned out to be the major alkaloids selected from *Phycella cyrtanthoides* bulbs and leaves extracts according to the UHPLC chromatogram (Figure 2). Docking experiments were performed to determine the pharmacological behavior of these main alkaloids, and therefore, their contributions to the cholinesterase inhibitory activities. The best docking binding energies expressed in kcal/mol of each selected compound are shown in Table 3.

Table 3. Binding energies obtained from docking experiments of selected major alkaloids in *Phycella cyrtanthoides* bulbs and leaves extracts, as well as the known inhibitor galanthamine over acetylcholinesterase (*TcAChE*) and butyrylcholinesterase (*hBChE*).

Compound	Binding Energy (kcal/mol) Acetylcholinesterase	Binding Energy (kcal/mol) Butyrylcholinesterase
3-hydroxydihydrocaranine (13)	−8.67	−8.06
Kirkine (25)	−8.42	−8.33
10- <i>O</i> -dimethylgalanthine (31)	−8.27	−7.1
2- α -methoxy-6- <i>O</i> -ethyloduline (22)	−9.38	−8.21
10-norpluviine (24)	−8.56	−7.48
3- <i>O</i> -acetylnarcissidine (30)	−8.88	−7.68
Galanthamine	−11.81	−9.5

3.3.1. Acetylcholinesterase (*TcAChE*) Docking Results

The binding energies shown in Table 3 indicate that 2- α -methoxy-6-*O*-ethyloduline is the main compound responsible for acetylcholinesterase inhibition, even though all derivatives displayed good binding energies over the enzyme, such as 3-*O*-acetylnarcissidine and 3-hydroxydihydrocaranine, which showed energy descriptors of −8.88 kcal/mol and −8.67 kcal/mol, respectively, turning them into good candidates as acetylcholinesterase inhibitors. These results are consistent with the experimental data that showed both bulbs and leaves extracts demonstrated good half-maximal inhibitory concentration (IC₅₀ values were within the same order of magnitude in µg/mL), as depicted in Table 2.

The docking assays indicated that all the main alkaloids that are reported in the present study establish hydrogen bond interactions with acetylcholinesterase. In addition to the hydrogen bond interactions, some alkaloids also establish π - π interactions, T-shaped interactions, and salt bridges. For instance, 3-hydroxydihydrocaranine performs the following interactions with acetylcholinesterase: one π - π interaction between the benzene ring of Phe330 and the 1,3-benzodioxole moiety, and two hydrogen bond interactions (one of which occurs between the Glu199 carboxylate group (−COOH) and one of its secondary

alcohols (–OH), while the other hydrogen bond interaction occurs between another secondary –OH and the amino acid Ser200 of the acetylcholinesterase catalytic site), as depicted in Figure 4A. Kirkine, as well as 3-hydroxydihydrocaranine, show one π – π interaction with Trp84, and two hydrogen bond interactions with Ser122 and Glu199, respectively (Figure 5B). The compound 10-norpluviine is arranged in a similar manner compared to Kirkine, both having their phenyl moieties of the 2-methoxyphenol frameworks overlapped between them in the enzyme’s catalytic site, leaving the tertiary amino groups of both compounds in opposite directions. This way, 10-norpluviine cannot perform a π – π interaction with Trp84, but instead still shows a good binding energy since it exhibits two hydrogen bond interactions with Tyr130 and through the carbonyl group (C=O) of Trp84. Additionally, 10-norpluviine exhibits a salt bridge with Asp72, which probably contributes to its binding stabilization into the enzyme catalytic site (Figure 5E). 3-*O*-acetylnarcissidine displays an analogous pose into the acetylcholinesterase catalytic site with Kirkine and 10-norpluviine, but the 1,2-dimethoxybenzene core of 3-*O*-acetylnarcissidine is superimposed with the cycloaliphatic rings of the former compounds, performing two hydrogen bond interactions with Gly118 and Asp72, as well as a π – π interaction with Phe330 (Figure 5F).

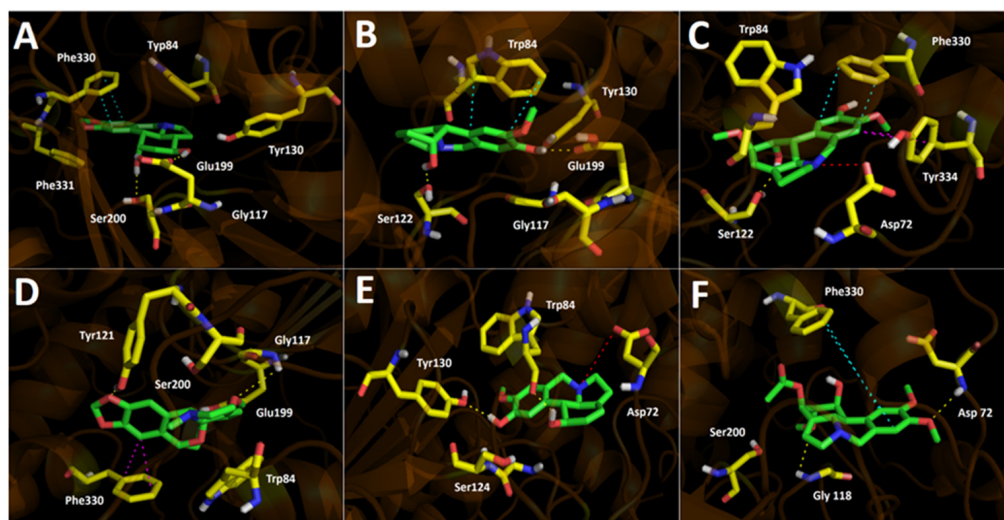


Figure 5. Predicted binding mode and predicted intermolecular interactions of major alkaloids in leaves and bulbs of *Phycella cyrtanthoides* extracts and the residues of *Torpedo californica* acetylcholinesterase (*TcAChE*) catalytic site; (A) 3-hydroxydihydrocaranine in the catalytic site; (B) Kirkine in the catalytic site; (C) 10-*O*-dimethylgalanthine in the catalytic site; (D) 2- α -methoxy-6-*O*-ethyloduline in the catalytic site; (E) 10-norpluviine in the catalytic site; (F) 3-*O*-acetylnarcissidine in the catalytic site. Yellow dotted lines indicate hydrogen bond interactions; cyan dotted lines represent π – π interactions; magenta dotted lines represent T-shaped interactions; and red dotted lines indicate salt bridge interactions.

10-*O*-dimethylgalanthine showed a good binding energy of -9.38 kcal/mol. Inside the acetylcholinesterase catalytic site, this derivative performs an important salt bridge interaction between the amino group and Asp72 amino acid, but also carries out a hydrogen bond interaction with Ser122, as well as π – π and T-shaped interactions through its aromatic 2-methoxyphenol moiety and the residues Phe330 and Tyr334, respectively. Therefore, these data confirm 10-*O*-dimethylgalanthine as a good candidate for acetylcholinesterase binding and inhibition (Figure 5C).

2- α -methoxy-6-*O*-ethyloduline, which demonstrated to possess the best binding energy of all derivatives, presents a slightly different binding mode in the acetylcholinesterase catalytic site compared to 3-hydroxydihydrocaranine. Notwithstanding, both compounds share the same direction of their 1,3-benzodioxole cores and their tertiary amino groups. However, the difference in the binding orientation of the 2- α -methoxy-6-*O*-ethyloduline

allows it to execute two hydrogen bond interactions with Glu199 and Tyr121, as well as a T-shaped interaction with Phe330, suggesting that these features are presumably responsible for the better binding energy profile (Figure 5D).

3.3.2. Butyrylcholinesterase (*h*BuChE) Docking Results

The binding energies from the docking assays of the major selected alkaloids from the *Phycella cyrtanthoides* extracts over butyrylcholinesterase also showed good binding energy profiles (Table 3). The half-maximal inhibitory concentration values (IC_{50}) for *P. cyrtanthoides* bulbs and *P. cyrtanthoides* leaves extracts were $18.32 \pm 0.03 \mu\text{g/mL}$ and $37.70 \pm 0.02 \mu\text{g/mL}$, respectively, indicating that they effectively inhibit the human butyrylcholinesterase. In this manner, the docking experiments confirm the inhibitory potential mentioned above. Kirkine was the alkaloid that exhibited the best binding energy (-8.33 kcal/mol). Kirkine displays three hydrogen bond interactions, two of which are performed by the hydroxyl group ($-\text{OH}$) of its 2-methoxyphenol moiety, where the hydrogen atom of the $-\text{OH}$ interacts with the carboxylate group of Glu197, whereas the oxygen atom of the same $-\text{OH}$ interacts with Ser198. The third hydrogen bond interaction occurs between the secondary alcohol ($-\text{OH}$) present in one of the cycloaliphatic rings of Kirkine and the amino acid His438 (Figure 6B). Furthermore, the same 2-methoxyphenol aromatic ring of Kirkine is in charge to perform other two T-shaped interactions with the residues Trp82 and His438, whereupon this alkaloid derivative achieves good stability within the butyrylcholinesterase catalytic site (Figure 6B). In the same way, 10-norpluviine is arranged in a similarly mode into the enzyme pocket; in fact, the same hydrogen bond interactions with Glu197, Ser 198 and His438, as well as the T-shaped interaction with His438 could be perceived (Figure 6E). Nonetheless, this derivative does not perform the T-shaped interaction seen in Kirkine with Trp82, which could explain the lower energy shown for 10-norpluviine (Table 3). 10-*O*-dimethylgalanthine is positioned in an opposite manner relative to Kirkine and 10-norpluviine; therefore, the interactions performed by 10-*O*-dimethylgalanthine are executed with different residues of the catalytic cavity, showing two hydrogen bond interactions with Ala328 and His438, one π -cation interaction between the amino group and Trp82, as well as a salt bridge with the latter amino group and Glu197 (Figure 6C).

3-hydroxydihydrocaranine carries out three hydrogen bond interactions with the amino acids Asp72, Trp82 and Tyr128. Moreover, 3-hydroxydihydrocaranine shares a relatively common binding pose with 3-*O*-acetylnarcissidine into the butyrylcholinesterase catalytic site. Nonetheless, the fact that these two derivatives show similar, but not identical, orientations results in a common hydrogen bond interaction with the amino acid Asp70. A hydrogen bond interaction through one of the oxygen atoms of the 1,3-benzodioxole framework in the case of 3-hydroxydihydrocaranine, and the same hydrogen bond interaction through one of the oxygen atoms of the 1,2-dimethoxybenzene core of 3-*O*-acetylnarcissidine. Likewise, 3-*O*-acetylnarcissidine also carries out another hydrogen bond interaction with Ser198 and the only methoxy group ($-\text{OCH}_3$) of its structure, which is present in one of its cycloaliphatic rings (Figure 6A,F).

The 2- α -methoxy-6-*O*-ethyloduline established pose into the butyrylcholinesterase catalytic site is quite different relative to the other major alkaloids studied; however, this derivative is still stabilized through two hydrogen bond interactions with Gly116 and Ser198, as well as two T-shaped interactions performed by the 1,3-benzodioxole moiety and the amino acids Trp82 and His438 (Figure 6D).

3.4. Antiproliferative Effects

The antiproliferative effects of bulbs and leaves of *P. cyrtanthoides* alkaloid extracts were tested in the following six tumor cell lines: A549 (lung), HBL-100 (breast), HeLa (cervix), SW1573 (lung), T-47D (breast) and WiDr (colon). To the best of our knowledge, no previous studies regarding the antiproliferative potential have been conducted on *Phycella* genera. The alkaloid extracts showed activity against all tumor cell lines in this study. Both

extracts display a GI_{50} (50% growth inhibition) $<2.5 \mu\text{g/mL}$ against all cell lines. These results indicate that the potency of the compounds present in the extract is comparable to standard anticancer drugs. For instance, cisplatin under the same six cell lines displayed GI_{50} values in the range $0.54\text{--}6.9 \mu\text{g/mL}$ (Table S1, Supplementary Material). Additionally, several alkaloids contained in the extracts have been previously identified to have anticancer activity. Lycorine showed significant antiproliferative effects against A2780 and MV4-11 cells [55]. Previous studies have demonstrated that lycorine and haemanthamine were able to inhibit cell proliferation using a panel of 16 tumor cell lines [5]. In a previous report, some alkaloids, such as norpluviine, caranine, dihydrolycorine, pseudolycorine, and lycorine, were also investigated against A549, OE21, Hs683, U373, SKMEL, and B16F10 cancer cell lines [56]. In addition, from *Hippeastrum solandriflorum*, several isolated alkaloids, including narcissidine, 11-hydroxyvittatine, narciclasine, among others, were evaluated against HCT-116 (colon adenocarcinoma), HL-60 (leukemia), OVCAR-8 (ovarian carcinoma) and SF-295 (glioblastoma) cancer cell lines [57]. On the other hand, the homolycorine-type alkaloid hippeastrine inhibited the proliferation of Hep G2 and HT-29 cells [37]. In addition, albomaculine have been evaluated against breast (Hs578T, MDA-MB-231, MCF7), colon (HCT-15), melanoma (SK-MEL-28) and lung (A549) cells lines [43]. Lycorine and homolycorine-type alkaloids were the most common alkaloids identified in *P. cyrthanthoides*, which could be strongly associated as the main compounds responsible for the antiproliferative effects.

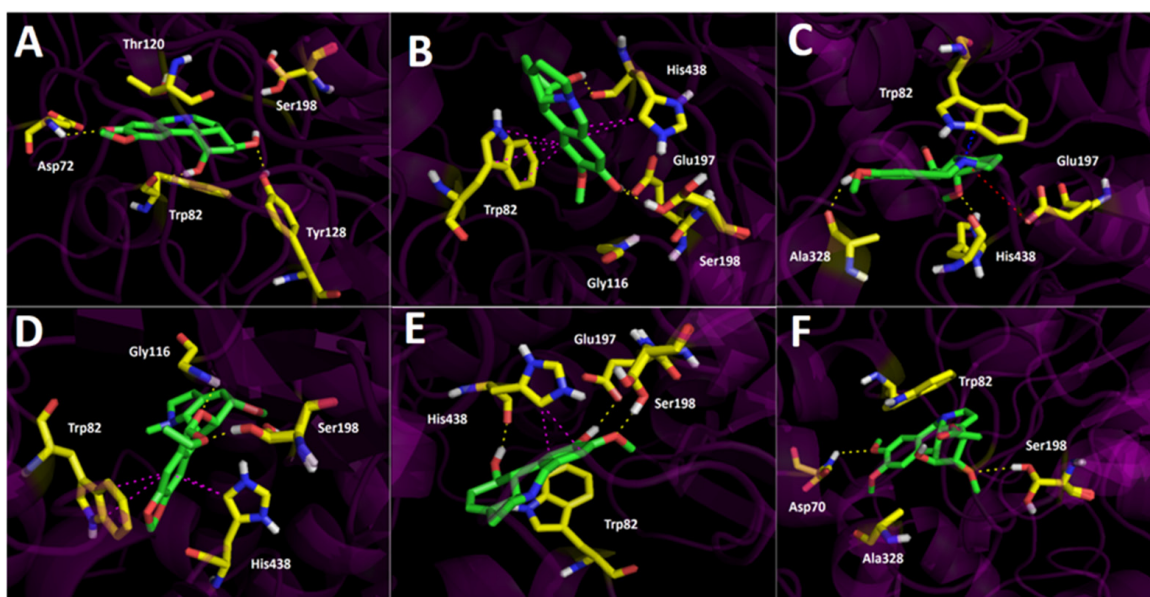


Figure 6. Predicted binding mode and predicted intermolecular interactions of major alkaloids in leaves and bulbs *Phycella cyrthanthoides* extracts and the residues of the human butyrylcholinesterase (*hBuChE*) catalytic site; (A) 3-hydroxydihydrocaranine in the catalytic site; (B) Kirkine in the catalytic site; (C) 10-*O*-dimethylgalanthine in the catalytic site; (D) 2- α -methoxy-6-*O*-ethyloduline in the catalytic site; (E) 10-norpluviine in the catalytic site; (F) 3-*O*-acetylnarcissidine in the catalytic site. Yellow dotted lines indicate hydrogen bond interactions; cyan dotted lines represent π - π interactions; magenta dotted lines represent T-shaped interactions; blue dotted lines indicate π -cation interactions; and red dotted lines indicate salt bridge interactions.

4. Conclusions

In summary, seventy alkaloids were detected in bulbs and leaves from the endemic Amaryllidaceae plant *Phycella cyrthanthoides* using UHPLC-DAD-Orbitrap-MS mass spectrometry analysis. Lycorine and haemanthamine type were the major alkaloids identified. The alkaloids extract showed activity against AChE and BChE, but no activity was observed against tyrosinase enzymes. Bulbs' extracts proved to be the most active against

both cholinesterase enzymes. The docking results indicated that hydrogen bond and T-shaped interactions are responsible for better binding over AChE and BChE enzymes. The assessment of the antiproliferative activity indicates that bulbs and leaves exert activity against several human tumor cell lines. The results reported herein are promising and indicate that alkaloid compounds that are present in *Phycella cyrtanthoides* extracts should be further studied for their antiproliferative activities as well as their potential therapeutic applications against neurodegenerative diseases. However, the isolation of major alkaloids as well as *in vivo* studies are needed to further evaluate the pharmacological properties of this plant.

Supplementary Materials: The following are available online at <https://www.mdpi.com/article/10.3390/metabo12020188/s1>, Figure S1: Alkaloids subjected to docking assays in the corresponding catalytic sites of *Torpedo californica* acetylcholinesterase (*TcAChE*) and human butyrylcholinesterase (*hBuChE*), Table S1. Antiproliferative activity (GI₅₀, in µg/mL) of *P. cyrtanthoides*, against human solid tumor cell lines.

Author Contributions: M.J.S. and C.F.-G. conceived and designed the experiments and wrote the paper; C.F.-G. performed the enzymatic experiments; M.J.S. and C.F.-G. analyzed the data of HPLC/MS. J.R.-P. performed the docking studies and wrote the results. A.P. and J.M.P. performed the antiproliferative experiments. All authors have read and agreed to the published version of the manuscript.

Funding: C.F.-G. acknowledges Postdoctorado FONDECYT 3190794. Financial support was provided by FONDECYT 1180059 and 1220075 to M.J.S. and 3190794 to C.F.-G. A.P. and J.M.P. thank the Canary Islands Government (grants EIS 2020 06_ULL and ProID2020010101, ACIISI/FEDER, UE) for financial support. A.P. thanks the EU Social Fund (FSE) and the Canary Islands ACIISI for the predoctoral grant TESIS2020010055.

Institutional Review Board Statement: Not applicable.

Informed Consent Statement: Not applicable.

Data Availability Statement: Data is contained within the article or Supplementary Material. The raw UHPLC MS data or other additional data presented in this study are available on request from the corresponding author.

Acknowledgments: C.F.-G. wishes to thank Ernane Souza for the critical reading and corrections.

Conflicts of Interest: The authors declare no conflict of interest. The funding sponsors had no role in the design of the study; in the collection, analysis, and interpretation of data; in the writing of the manuscript; or in the decision to publish the results.

References

1. He, M.; Qu, C.; Gao, O.; Hu, X.; Hong, X. Biological and pharmacological activities of Amaryllidaceae alkaloids. *RSC Adv.* **2015**, *5*, 16562–16574. [[CrossRef](#)]
2. Riddle, J.M. Ancient and medieval chemotherapy for cancer. *Isis* **1985**, *76*, 319–330. [[CrossRef](#)] [[PubMed](#)]
3. Van Goietsenoven, G.; Mathieu, V.; Lefranc, F.; Kornienko, A.; Evidente, A.; Kiss, R. Narciclasine as well as other Amaryllidaceae Isocarbostryls are Promising GTP-ase Targeting Agents against Brain Cancers. *Med. Res. Rev.* **2013**, *33*, 439–455. [[CrossRef](#)] [[PubMed](#)]
4. Heo, J.H.; Eom, B.H.; Ryu, H.W.; Kang, M.G.; Park, J.E.; Kim, D.Y.; Kim, J.H.; Park, D.; Oh, S.R.; Kim, H. Acetylcholinesterase and butyrylcholinesterase inhibitory activities of khellactone coumarin derivatives isolated from *Peucedanum japonicum* Thurnberg. *Sci. Rep.* **2020**, *10*, 21695. [[CrossRef](#)] [[PubMed](#)]
5. Havelek, R.; Muthna, D.; Tomsik, P.; Kralovec, K.; Seifrtova, M.; Cahlikova, L.; Hostalkova, A.; Safratova, M.; Perwein, M.; Cermakova, E.; et al. Anticancer potential of Amaryllidaceae alkaloids evaluated by screening with a panel of human cells, real-time cellular analysis and Ehrlich tumor-bearing mice. *Chem. Biol. Interact.* **2017**, *275*, 121–132. [[CrossRef](#)]
6. Yu, H.; Qiu, Y.; Pang, X.; Li, J.; Wu, S.; Yin, S.; Han, L.; Zhang, Y.; Jin, C.; Gao, X.; et al. Lycorine Promotes Autophagy and Apoptosis via TCRP1/Akt/mTOR Axis Inactivation in Human Hepatocellular Carcinoma. *Mol. Cancer. Ther.* **2017**, *16*, 2711–2723. [[CrossRef](#)]
7. Cahliková, L.; Kawano, I.; Řezáčová, M.; Blunden, G.; Hulcová, D.; Havelek, R. The Amaryllidaceae alkaloids haemanthamine, haemanthidine and their semisynthetic derivatives as potential drugs. *Phytochem. Rev.* **2021**, *20*, 303–323. [[CrossRef](#)]
8. Griffin, C.; Sharda, N.; Sood, D.; Nair, J.; McNulty, J.; Pandey, S. Selective cytotoxicity of Pancratistatin-related natural Amaryllidaceae alkaloids: Evaluation of the activity of two new compounds. *Cancer Cell Int.* **2007**, *7*, 10. [[CrossRef](#)]

9. Evidente, A.; Andolfi, A.; Abou-Donia, A.H.; Touema, S.M.; Hammouda, H.M.; Shawky, E.; Motta, A. (-)-Amarbellisine, a lycorine-type alkaloid from *Amaryllis belladonna* L. growing in Egypt. *Phytochemistry* **2004**, *65*, 2113–2118. [[CrossRef](#)]
10. Deng, B.; Ye, L.; Yin, H.; Liu, Y.; Hu, S.; Li, B. Determination of pseudolycorine in the bulb of *Lycoris radiata* by capillary electrophoresis combined with online electrochemiluminescence using ultrasonic-assisted extraction. *J. Chromatogr. B Analyt. Technol. Biomed. Life Sci.* **2011**, *879*, 927–932. [[CrossRef](#)]
11. Zhang, Y.; Chen, Z. Nonaqueous CE ESI-IT-MS analysis of Amaryllidaceae alkaloids. *J. Sep. Sci.* **2013**, *36*, 1078–1084. [[CrossRef](#)] [[PubMed](#)]
12. Tallini, L.R.; Bastida, J.; Cortes, N.; Osorio, E.H.; Theoduloz, C.; Schmeda-Hirschmann, G. Cholinesterase inhibition activity, alkaloid profiling and molecular docking of Chilean *Rhodophiala* (Amaryllidaceae). *Molecules* **2018**, *23*, 1532. [[CrossRef](#)] [[PubMed](#)]
13. Petruczynik, A.; Misiurek, J.; Tuzimski, T.; Uszyński, R.; Szymczak, G.; Chernetsky, M.; Waksmundzka-Hajnos, M. Comparison of different HPLC systems for analysis of galantamine and lycorine in various species of Amaryllidaceae family. *J. Liq. Chromatogr. Relat. Technol.* **2016**, *39*, 574–579. [[CrossRef](#)]
14. Ortiz, J.E.; Pigni, N.B.; Andujar, S.A.; Roitman, G.; Suvire, F.D.; Enriz, R.D.; Tapia, A.; Bastida, J.; Feresin, G.E. Alkaloids from *Hippeastrum argentinum* and Their Cholinesterase-Inhibitory Activities: An in Vitro and in Silico Study. *J. Nat. Prod.* **2016**, *79*, 1241–1248. [[CrossRef](#)]
15. Karakoyun, Ç.; Bozkurt, B.; Çoban, G.; Masi, M.; Cimmino, A.; Evidente, A.; Unver Somer, N. A comprehensive study on *Narcissus tazetta* subsp. *tazetta* L.: Chemo-profiling, isolation, anticholinesterase activity and molecular docking of Amaryllidaceae alkaloids. *S. Afr. J. Bot.* **2020**, *130*, 148–154. [[CrossRef](#)]
16. Li, A.; Du, Z.; Liao, M.; Feng, Y.; Ruan, H.; Jiang, H. Discovery and characterisation of lycorine-type alkaloids in *Lycoris* spp. (Amaryllidaceae) using UHPLC-QTOF-MS. *Phytochem. Anal.* **2019**, *30*, 268–277. [[CrossRef](#)]
17. Jin, Z. Amaryllidaceae and *Scelletium* alkaloids. *Nat. Prod. Rep.* **2013**, *30*, 849–868. [[CrossRef](#)]
18. Baeza, C.; Ruiz, E.; Almendras, F.; Peñailillo, P. Estudio comparativo del cariotipo en especies de *Miltinea* Ravenna, *Phycella* Lindl. y *Rhodophiala* C. Presl (Amaryllidaceae) de Chile. *Rev. Fac. Cienc. Agrar.* **2012**, *44*, 193–205.
19. Cisternas, M.A.; Araneda, L.; García, N.; Baeza, C.M. Estudios cariotípicos en el género chileno *Placea* (Amaryllidaceae). *Gayana Bot.* **2010**, *67*, 198–205. [[CrossRef](#)]
20. Urbina-Casanova, R.; Saldivia, P.; Scherson, R.A. Consideraciones sobre la sistemática de las familias y los géneros de plantas vasculares endémicos de Chile. *Gayana Bot.* **2015**, *72*, 272–295. [[CrossRef](#)]
21. García, N.; Meerow, A.W.; Arroyo-Leuenberger, S.; Oliveira, R.S.; Dutilh, J.H.; Soltis, P.S.; Judd, W.S. Generic classification of Amaryllidaceae tribe Hippeastreae. *TAXON* **2019**, *68*, 481–498. [[CrossRef](#)]
22. Trujillo-Chacón, L.M.; Alarcón-Enos, J.E.; Céspedes-Acuña, C.L.; Bustamante, L.; Baeza, M.; López, M.G.; Fernández-Mendivil, C.; Cabezas, F.; Pastene-Navarrete, E.R. Neuroprotective activity of isoquinoline alkaloids from Chilean Amaryllidaceae plants against oxidative stress-induced cytotoxicity on human neuroblastoma SH-SY5Y cells and mouse hippocampal slice culture. *Food Chem. Toxicol.* **2019**, *132*, 110665. [[CrossRef](#)] [[PubMed](#)]
23. Ortiz, J.E.; Berkov, S.; Pigni, N.B.; Theoduloz, C.; Roitman, G.; Tapia, A.; Bastida, J.; Feresin, G.E. Wild argentinian Amaryllidaceae, a new renewable source of the acetylcholinesterase inhibitor galanthamine and other alkaloids. *Molecules* **2012**, *17*, 13473–13482. [[CrossRef](#)]
24. Reis, A.; Magne, K.; Massot, S.; Tallini, L.R.; Scopel, M.; Bastida, J.; Ratet, P.; Zuanazzi, J.A.S. Amaryllidaceae alkaloids: Identification and partial characterization of montanine production in *Rhodophiala bifida* plant. *Sci. Rep.* **2019**, *9*, 8471. [[CrossRef](#)] [[PubMed](#)]
25. Barrientos, R.; Fernández-Galleguillos, C.; Pastene, E.; Simirgiotis, M.; Romero-Parra, J.; Ahmed, S.; Echeverría, J. Metabolomic Analysis, Fast Isolation of Phenolic Compounds, and Evaluation of Biological Activities of the Bark from *Weinmannia trichosperma* Cav. (Cunoniaceae). *Front. Pharmacol.* **2020**, *11*, 780. [[CrossRef](#)] [[PubMed](#)]
26. Fernández-Galleguillos, C.; Quesada-Romero, L.; Puerta, A.; Padrón, J.M.; Souza, E.; Romero-Parra, J.; Simirgiotis, M.J. UHPLC-MS chemical fingerprinting and antioxidant, antiproliferative, and enzyme inhibition potential of *Gaultheria pumila* berries. *Metabolites* **2021**, *11*, 523. [[CrossRef](#)]
27. Larrazabal-Fuentes, M.J.; Fernández-Galleguillos, C.; Palma-Ramírez, J.; Romero-Parra, J.; Sepúlveda, K.; Galetovic, A.; González, J.; Paredes, A.; Bórquez, J.; Simirgiotis, M.J.; et al. Chemical Profiling, Antioxidant, Anticholinesterase, and Antiprotozoal Potentials of *Artemisia copa* Phil. (Asteraceae). *Front. Pharmacol.* **2020**, *11*, 1911. [[CrossRef](#)]
28. Barrientos, R.E.; Ahmed, S.; Cortés, C.; Fernández-Galleguillos, C.; Romero-Parra, J.; Simirgiotis, M.J.; Echeverría, J. Chemical Fingerprinting and Biological Evaluation of the Endemic Chilean Fruit *Greigia sphacelata* (Ruiz and Pav.) Regel (Bromeliaceae) by UHPLC-PDA-Orbitrap-Mass Spectrometry. *Molecules* **2020**, *25*, 3750. [[CrossRef](#)]
29. Petersson, G.A.; Bennett, A.; Tensfeldt, T.G.; Al-Laham, M.A.; Shirley, W.A.; Mantzaris, J. A complete basis set model chemistry. I. The total energies of closed-shell atoms and hydrides of the first-row elements. *J. Chem. Phys.* **1988**, *89*, 2193–2218. [[CrossRef](#)]
30. McLean, A.D.; Chandler, G.S. Contracted Gaussian basis sets for molecular calculations. I. Second row atoms, Z = 11–18. *J. Chem. Phys.* **2008**, *72*, 5639. [[CrossRef](#)]
31. Greenblatt, H.M.; Kryger, G.; Lewis, T.; Silman, I.; Sussman, J.L. Structure of acetylcholinesterase complexed with (-)-galanthamine at 2.3 Å resolution. *FEBS Lett.* **1999**, *463*, 321–326. [[CrossRef](#)]

32. Nachon, F.; Carletti, E.; Ronco, C.; Trovaslet, M.; Nicolet, Y.; Jean, L.; Renard, P.Y. Crystal structures of human cholinesterases in complex with huprine W and tacrine: Elements of specificity for anti-Alzheimer's drugs targeting acetyl- and butyrylcholinesterase. *Biochem. J.* **2013**, *453*, 393–399. [[CrossRef](#)] [[PubMed](#)]
33. Berman, H.M.; Westbrook, J.; Feng, Z.; Gilliland, G.; Bhat, T.N.; Weissig, H.; Shindyalov, I.N.; Bourne, P.E. The Protein Data Bank. *Nucleic Acids Res.* **2000**, *28*, 235–242. [[CrossRef](#)] [[PubMed](#)]
34. Shitara, N.; Hirasawa, Y.; Hasumi, S.; Sasaki, T.; Matsumoto, M.; Wong, C.P.; Kaneda, T.; Asakawa, Y.; Morita, H. Four new Amaryllidaceae alkaloids from *Zephyranthes candida*. *J. Nat. Med.* **2014**, *68*, 610–614. [[CrossRef](#)]
35. Cortes, N.; Sierra, K.; Alzate, F.; Osorio, E.H.; Osorio, E. Alkaloids of Amaryllidaceae as Inhibitors of Cholinesterases (AChEs and BChEs): An Integrated Bioguided Study. *Phytochem. Anal.* **2018**, *29*, 217–227. [[CrossRef](#)] [[PubMed](#)]
36. Katoch, D.; Kumar, D.; Padwad, Y.S.; Singh, B.; Sharma, U. Pseudolycorine N-oxide, a new N-oxide from *Narcissus tazetta*. *Nat. Prod. Res.* **2019**, *34*, 2051–2058. [[CrossRef](#)]
37. Chen, G.-L.; Tian, Y.-Q.; Wu, J.-L.; Li, N.; Guo, M.-Q. Antiproliferative activities of Amaryllidaceae alkaloids from *Lycoris radiata* targeting DNA topoisomerase I. *Sci. Rep.* **2016**, *6*, 38284. [[CrossRef](#)]
38. De Andrade, J.P.; Guo, Y.; Font-Bardia, M.; Calvet, T.; Dutilh, J.; Viladomat, F.; Codina, C.; Nair, J.J.; Zuanazzi, J.A.S.; Bastida, J. Crinine-type alkaloids from *Hippeastrum aulicum* and *H. calyptratum*. *Phytochemistry* **2014**, *103*, 188–195. [[CrossRef](#)]
39. Zhang, X.; Huang, H.; Liang, X.; Huang, H.; Dai, W.; Shen, Y.; Yan, S.; Zhang, W. Analysis of Amaryllidaceae alkaloids from *Crinum* by high-performance liquid chromatography coupled with electrospray ionization tandem mass spectrometry. *Rapid Commun. Mass Spectrom.* **2009**, *23*, 2903–2916. [[CrossRef](#)]
40. Giordani, R.B.; Vieira, P.D.B.; Weizenmann, M.; Rosemberg, D.B.; Souza, A.P.; Bonorino, C.; De Carli, G.A.; Bogo, M.R.; Zuanazzi, J.A.; Tasca, T. Candimine-induced cell death of the amitochondriate parasite *Trichomonas vaginalis*. *J. Nat. Prod.* **2010**, *73*, 2019–2023. [[CrossRef](#)]
41. Cortes, N.; Castañeda, C.; Osorio, E.H.; Cardona-Gomez, G.P.; Osorio, E. Amaryllidaceae alkaloids as agents with protective effects against oxidative neural cell injury. *Life Sci.* **2018**, *203*, 54–65. [[CrossRef](#)] [[PubMed](#)]
42. Huang, S.D.; Zhang, Y.; He, H.P.; Li, S.F.; Tang, G.H.; Chen, D.Z.; Cao, M.M.; Di, Y.T.; Hao, X.J. A new Amaryllidaceae alkaloid from the bulbs of *Lycoris radiata*. *Chin. J. Nat. Med.* **2013**, *11*, 406–410. [[CrossRef](#)] [[PubMed](#)]
43. Masi, M.; Van slambrouck, S.; Gunawardana, S.; van Rensburg, M.J.; James, P.C.; Mochel, J.G.; Heliso, P.S.; Albalawi, A.S.; Cimmino, A.; van Otterlo, W.A.L.; et al. Alkaloids isolated from *Haemanthus humilis* Jacq., an indigenous South African Amaryllidaceae: Anticancer activity of coccinine and montanine. *S. Afr. J. Bot.* **2019**, *126*, 277–281. [[CrossRef](#)]
44. Tarakemeh, A.; Azizi, M.; Rowshan, V.; Salehi, H.; Spina, R.; Dupire, F.; Arouie, H.; Laurain-Mattar, D. Screening of Amaryllidaceae alkaloids in bulbs and tissue cultures of *Narcissus papyraceus* and four varieties of *N. tazetta*. *J. Pharm. Biomed. Anal.* **2019**, *172*, 230–237. [[CrossRef](#)]
45. Quirion, J.C.; Husson, H.P.; Weniger, B.; Jimenez, F.; Zaroni, T.A. (-)-3-O-Acetylnarcissidine, a New Alkaloid from *Hippeastrum puniceum*. *J. Nat. Prod.* **2004**, *54*, 1112–1114. [[CrossRef](#)]
46. De Andrade, J.P.; Pigni, N.B.; Torras-Claveria, L.; Berkov, S.; Codina, C.; Viladomat, F.; Bastida, J. Bioactive alkaloid extracts from *Narcissus broussonetii*: Mass spectral studies. *J. Pharm. Biomed. Anal.* **2012**, *70*, 13–25. [[CrossRef](#)]
47. Pigni, N.B.; Ríos-Ruiz, S.; Martínez-Francés, V.; Nair, J.J.; Viladomat, F.; Codina, C.; Bastida, J. Alkaloids from *Narcissus serotinus*. *J. Nat. Prod.* **2012**, *75*, 1643–1647. [[CrossRef](#)]
48. Masi, M.; Frolova, L.V.; Yu, X.; Mathieu, V.; Cimmino, A.; De Carvalho, A.; Kiss, R.; Rogelj, S.; Pertsemelidis, A.; Kornienko, A.; et al. Jonquailine, a new pretazettine-type alkaloid isolated from *Narcissus jonquilla* quail, with activity against drug-resistant cancer. *Fitoterapia* **2015**, *102*, 41–48. [[CrossRef](#)]
49. Kaya, G.I.; Unver, N.; Gözler, B.; Bastida, J. (-)-Capnoidine and (+)-bulbocapnine from an Amaryllidaceae species, *Galanthus nivalis* subsp. *cilicicus*. *Biochem. Syst. Ecol.* **2004**, *32*, 1059–1062. [[CrossRef](#)]
50. Tallini, L.R.; de Andrade, J.P.; Kaiser, M.; Viladomat, F.; Nair, J.J.; Zuanazzi, J.A.S.; Bastida, J. Alkaloid Constituents of the Amaryllidaceae Plant *Amaryllis belladonna* L. *Molecules* **2017**, *22*, 1437. [[CrossRef](#)]
51. Al Mamun, A.; Maříková, J.; Hulcová, D.; Janoušek, J.; Šafratová, M.; Nováková, L.; Kučera, T.; Hrabínová, M.; Kuneš, J.; Korábečný, J.; et al. Amaryllidaceae Alkaloids of Belladine-Type from *Narcissus pseudonarcissus* cv. Carlton as New Selective Inhibitors of Butyrylcholinesterase. *Biomolecules* **2020**, *10*, 800. [[CrossRef](#)] [[PubMed](#)]
52. Van Rensburg, E.; Zietsman, P.C.; Bonnet, S.L.; Wilhelm, A. Alkaloids from the Bulbs of *Boophone disticha*. *Nat. Prod. Commun.* **2017**, *12*, 1431–1433. [[CrossRef](#)]
53. Ghosal, S.; Rao, P.H.; Saini, K.S. Natural Occurrence of 11-O-Acetylbambelline and 11-O-Acetyl-1,2-β-epoxybambelline in *Crinum latifolium*: Immuno-regulant Alkaloids. *Pharm. Res.* **1985**, *2*, 251–252. [[CrossRef](#)]
54. Cespedes, C.L.; Balbontin, C.; Avila, J.G.; Dominguez, M.; Alarcon, J.; Paz, C.; Burgos, V.; Ortiz, L.; Peñaloza-Castro, I.; Seigler, D.S.; et al. Inhibition on cholinesterase and tyrosinase by alkaloids and phenolics from *Aristolelia chilensis* leaves. *Food Chem. Toxicol.* **2017**, *109*, 984–995. [[CrossRef](#)] [[PubMed](#)]
55. Abebe, B.; Tadesse, S.; Hymete, A.; Bisrat, D. Antiproliferative Effects of Alkaloids from the Bulbs of *Crinum abyscincicum* Hochst. ExA. Rich. *Evid. Based Complement. Altern. Med.* **2020**, *2020*, 2529730. [[CrossRef](#)]

56. Lamoral-Theys, D.; Andolfi, A.; Van Goietsenoven, G.; Cimmino, A.; Le Calvé, B.; Wauthoz, N.; Mégalizzi, V.; Gras, T.; Bruyère, C.; Dubois, J.; et al. Lycorine, the Main Phenanthridine Amaryllidaceae Alkaloid, Exhibits Significant Antitumor Activity in Cancer Cells That Display Resistance to Proapoptotic Stimuli: An Investigation of Structure–Activity Relationship and Mechanistic Insight. *J. Med. Chem.* **2009**, *52*, 6244–6256. [[CrossRef](#)] [[PubMed](#)]
57. Carvalho, K.R.; Silva, A.B.; Torres, M.C.M.; Pinto, F.C.L.; Guimarães, L.A.; Rocha, D.D.; Silveira, E.R.; Costa-Lotufo, L.V.; Braz-Filho, R.; Pessoa, O.D.L. Cytotoxic Alkaloids from *Hippeastrum solandriflorum* Lindl. *J. Braz. Chem. Soc.* **2015**, *26*, 1976–1980. [[CrossRef](#)]